NeuroImage 52 (2010) 1654–1666

Contents lists available at ScienceDirect

NeuroImage

journal homepage: www.elsevier.com/locate/ynimg

Persistent posterior and transient anterior medial temporal lobe activity during navigation

Jian Xu [a,b], Hallvard R. Evensmoen [b], Hanne Lehn [a], Carl W.S. Pintzka [a], Asta K. Håberg [b,c,*]

[a] Department of Circulation and Medical Imaging, Norwegian University of Science and Technology (NTNU), Trondheim, Norway
[b] Department of Medical Imaging, St. Olav's Hospital, Trondheim, Norway
[c] Department of Neuroscience, Norwegian University of Science and Technology (NTNU), Trondheim, Norway

ARTICLE INFO

Article history:
Received 9 October 2009
Revised 31 March 2010
Accepted 26 May 2010
Available online 4 June 2010

Keywords:
Entorhinal cortex
Parahippocampal cortex
Hippocampus
Self-localization
Initial phase

ABSTRACT

A functional segregation along the posterior–anterior axis of the medial temporal lobe (MTL) has been suggested. In brief, it is thought that the posterior hippocampus represents environmental detail and/or encodes space, whereas the anterior part represents the environment more as a whole and/or subserves behavior. Different phases of navigation should thus recruit different structures within the MTL. Based on animal studies and neuroimaging data from humans, the initial phase of navigation, i.e., self-localization, target localization and path planning, should depend on the anterior MTL independent of upcoming navigational demands, whereas posterior MTL should be active throughout navigation. We tested this prediction using fMRI with navigation in a learned large-scale virtual office landscape with numerous complex landmarks under different navigational conditions.

The initial navigational phase specifically engaged the anterior MTL. Increased activity was found bilaterally in the rostral and caudal entorhinal cortex. This is, to our knowledge, the first report of entorhinal activity in virtual navigation detected in a direct comparison. Also bilateral anterior hippocampus and anterior parahippocampal cortex were significantly more active during the initial phase. Activity lasting throughout the navigational period was found in the right posterior hippocampus and parahippocampal cortex. Hippocampal activity for the entire navigation period was only detected when the virtual environment remained unaltered. Navigational success was positively correlated with activity in the anterior right hippocampus for the initial phase, and more posteriorly in the hippocampus for the whole navigation period. Plots of the BOLD signal time course demonstrated that activity in the anterior hippocampus was transient whereas activity in the posterior hippocampus peaked regularly throughout the entire navigation period.

These results support a functional segregation within the MTL with regard to navigational phases. The anterior MTL appears to complete associations related to the environment at large and provide a behavioral plan for navigation, whereas the posterior part keeps track of current location.

Introduction

The medial temporal lobe (MTL), which includes the hippocampus and the parahippocampal and entorhinal cortices, is pivotal for the ability to navigate (Bird and Burgess, 2008; Burgess et al., 2002; Moser et al., 2008; Spiers and Maguire, 2007b). Previous neuroimaging studies demonstrate that different regions within the MTL are recruited during navigation, depending on the specific nature of the task (Doeller et al., 2008; Jordan et al., 2004; Rauchs et al., 2008; Shipman and Astur, 2008; Spiers and Maguire, 2006; Wolbers et al., 2007). The aim of the present study was to examine neuronal activation during the initial phase of navigation, which involves self-localization, target localization and planning how to reach the target (Jeffery, 2007) compared to execution of the navigation plan.

Neuroimaging data have demonstrated increased activity in the anterior hippocampus during navigational planning and target localization (Shipman and Astur, 2008; Spiers and Maguire, 2006). Activity lasting throughout a navigation period has only been reported in the posterior hippocampus (Peigneux et al., 2004; Rauchs et al., 2008). These findings can be interpreted as reflecting differential sensitivity to spatial detail in the posterior and anterior hippocampus. Behavioral studies have shown that in the initial phase of navigation subjects first retrieve a global representation of the environment. Subsequently, subjects identify the target's location within this global representation, choose direction, and plan a route to reach the target (Hölscher et al., 2006; Spiers and Maguire, 2008). In the execution phase, subjects fill in the details in the environment as they proceed toward the target (Spiers and Maguire, 2008). Animal studies indicate that the environment is represented with increasing

* Corresponding author. Department of Neuroscience, Faculty of Medicine Norwegian University of Science and Technology (NTNU), 7489 Trondheim, Norway. Fax: +47 73551350.
E-mail address: asta.haberg@ntnu.no (A.K. Håberg).

1053-8119/$ – see front matter © 2010 Elsevier Inc. All rights reserved.
doi:10.1016/j.neuroimage.2010.05.074

scale along the posterior–anterior axis of the hippocampus, i.e., local spatial detail is represented posteriorly whereas the environment at large is represented anteriorly (Jung et al., 1994; Kjelstrup et al., 2008). It should also be noted that spatial memory in rats depends in particular on the posterior two-thirds of the hippocampus (Moser and Moser, 1998) and that the anterior part is suggested to show greater involvement in non-spatial functions like behavioral control (Bast et al., 2009) and/or reward (Royer et al., 2010). Together these results suggest that the initial phase of navigation depends on a global representation of the space to be traversed, which should be processed in the anterior hippocampus, while the execution phase seems to be devoted to processing local environmental detail related to the current position engendered by the posterior hippocampus.

The entorhinal cortex, which is localized to the anterior part of the MTL, may also be particularly engaged in the initial phase of navigation. Mental navigation, which shares features with navigational planning, has been shown with PET to increase entorhinal cortex activity (Ghaem et al., 1997; Mellet et al., 2000). fMRI studies have shown that entorhinal activity increases during retrieval of landmark sequences from learned routes (Janzen and Weststeijn, 2007) and correlates positively with increasing distance to target (Spiers and Maguire, 2007a). In the initial phase, the subject is the farthest from the target and utilizes a global representation of the environment to plan the path to it (Hölscher et al., 2006; Spiers and Maguire, 2008, 2006). This implies that entorhinal activity could be recruited specifically in the initial phase of navigation. Animal studies suggest that the entorhinal cortex provides both temporal and spatial context signals, as "a crude sketch of locations traversed in a route" (Eichenbaum and Lipton, 2008; Lipton et al., 2007). Such a sketch may be the equivalent to the global environmental representation that subjects use to find the direction and route toward the target, described by human subjects (Hölscher et al., 2006; Spiers and Maguire, 2008).

There are also indications of a functional segregation along the anterior–posterior axis of the parahippocampal cortex. Visuospatial scenes particularly engage for the posterior part of the parahippocampal cortex (Epstein, 2008), with less in the anterior part (Litman et al., 2009). The more complex the scenes are, the greater the ensuing activation in this region (Chai et al., 2010). Furthermore, the posterior parahippocampal cortex has been shown to support encoding of both objects and their locations, while the anterior parahippocampal cortex engenders memory for location (Buffalo et al., 2006; Sommer et al., 2005). Thus, the posterior parahippocampal cortex can be regarded as having a more perceptual role, involving processing of scenes and details in them, while the anterior parahippocampal cortex subserves spatial memory.

The human and animal studies reviewed above suggest that the anterior parts of the MTL, i.e., anterior hippocampus, entorhinal cortex and anterior parahippocampal cortex, subserve the initial phase of navigation, while the posterior MTL, i.e., the posterior hippocampus and the posterior parahippocampal cortex, is the main contributor in the execution phase. To test this hypothesis, the current study set out to identify the subregions in the MTL that support the initial phase of navigation compared to the execution phase. We further predicted that activity in the initial phase of navigation is independent of upcoming navigational demands, so navigation was performed under three different conditions. The previous findings reviewed above are suggestive of this distinction between the initial phase of navigation and execution of a navigational plan, but to the best of our knowledge, it remains to be tested directly. To this end, we designed a large-scale, realistic virtual office landscape with 56 complex landmarks (Fig. 1). Subjects were first familiarized with the environment through free exploration and structured learning. Next, brain activity was investigated with fMRI during navigation in the learned environment. Navigation occurred under different navigational conditions; navigation in an unaltered version of the learned environment (condition Normal) in the same environment but with all landmarks removed except the start and target landmarks (condition Without) or in an environment where everything was unaltered expect that the most direct routes between the start position and target landmark were blocked (condition Blocked). The participants were placed at new locations within the environment and presented with a new target landmark (Fig. 1) at the beginning of each trial, thus forcing the subjects to self-localize, localize target landmark and formulate a navigation plan.

Methods

Participants

Twenty men (21–30 years, mean = 24.2 years) with no history of neurological disorders, head trauma or current DSM-IV axis I diagnosis of psychiatric illness, including substance abuse, were recruited from the university campus. They were all right-handed, ascertained with the Edinburg Handedness Inventory with mean score of 89.7%. All participants provided written informed consent prior to participation and received 500 Norwegian kroner as reimbursement. The study was approved by the National Committee for Medical Research Ethics in Midt-Norge, Norway.

Virtual environment

The virtual environment was developed in collaboration with Terra Vision AS (Terra Vision, Trondheim, Norway) using Torque game engine (Garage Games, Eugene, Oregon, USA). The environment is 115.28×138.46 units of size, which corresponds to 62×74 m in "real life". Player moving speed was fixed at 3.73 U/s. The environment mimics the inside of a modern office building with rooms, corridors and open areas of various sizes, but it lacks exterior windows. All doors inside the environment are "locked", i.e., subjects are only allowed to navigate through the corridors and open areas. Fifty-six distinct landmarks made up of 195 objects and 60 pictures are placed at various locations (Fig. 1). Most of the landmarks comprised of several objects. All objects making up a complex landmark had a common theme. Wall structure, ceiling, carpeting and lighting of the interior were similar throughout the environment and modeled to make it as realistic as possible.

Pre-scanning

Using a standard desktop computer and a sidewinder pro joystick (Logitech, Romanel-sur-Morges, Switzerland), participants first explored the virtual environment freely in two 12-min sessions. After the second free exploration session, participants performed structured navigation tasks. This was done in order to ensure that all subjects had seen every landmark. In all these navigation tasks, all starting landmarks and target landmarks were positioned in the east-west direction of each other. Task order was randomized between subjects. Participants were given a maximum of 60 min to complete the structured learning session.

Subsequently, the participants performed three computer-based tests to ascertain their level of proficiency of the virtual environment: recognition of landmarks, judgments of distance and judgments of direction between landmarks.

Finally participants were given a brief demonstration of each task condition in the fMRI experiment and practiced one of each task type. Before MRI, participants were given a 30-min break.

Scanning procedure

Scanning was performed on a 3-T Siemens Trio scanner with a 12-channel Head Matrix Coil (Siemens AG, Erlangen, Germany). Foam

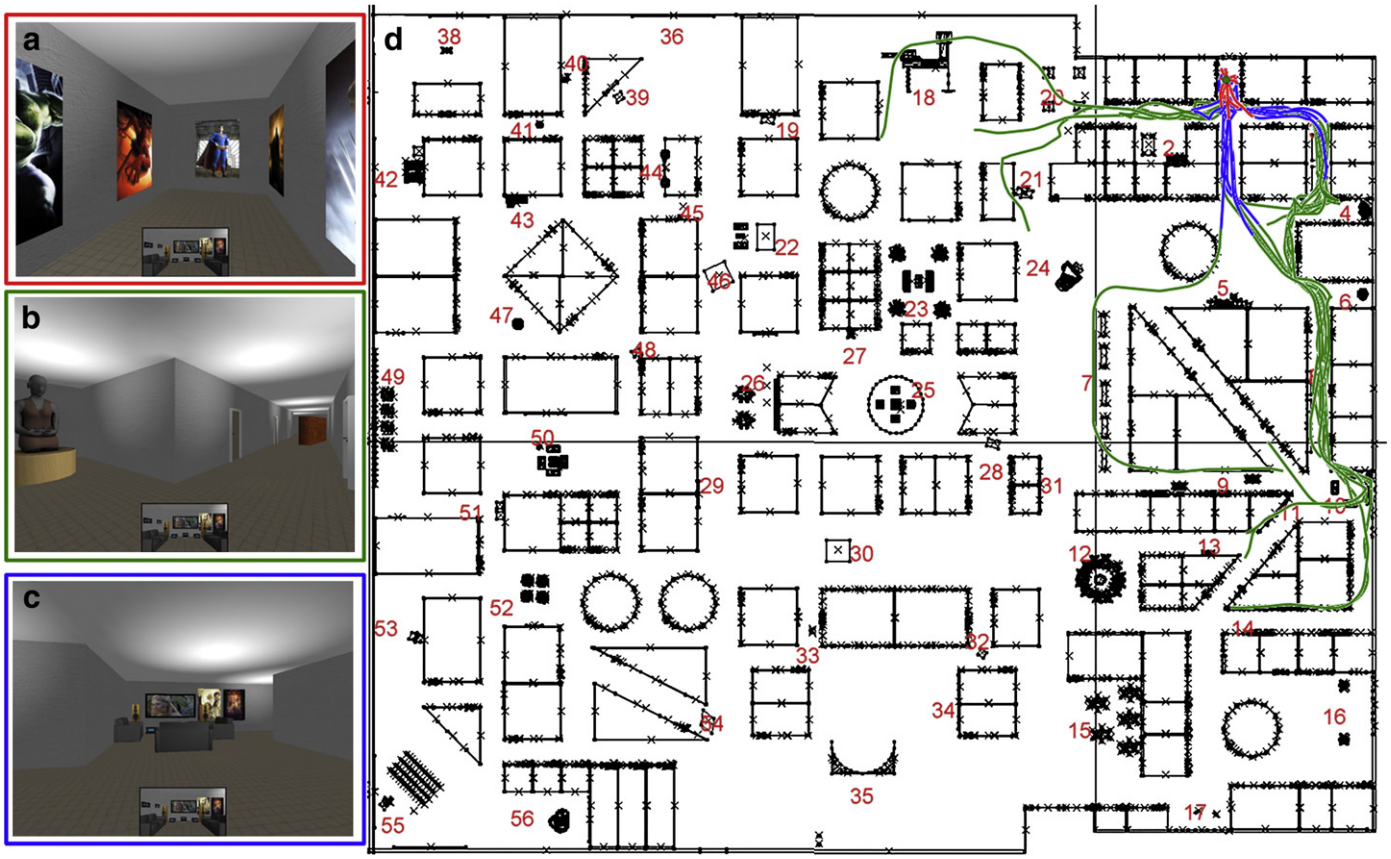

Fig. 1. Overview of the virtual environment. (a) The initial view presented to the participant when entering at a random location within the virtual environment at the start of each new navigation block. The target landmark was shown as a small image in the middle, bottom of the screen. The initial phase consisting of self-localization, target localization and path planning were determined from participants' post-scan self-reports to last 4.6 s. The movements for all 18 participants during the initial 4.6 s are marked as red lines on the map of the virtual environment to the right in the figure. (b) View of the environment as the participants moved toward the target in the phase directly following the initial phase. The movements of all participants during the subsequent 4.6 s following the initial phase are represented as blue lines in the map of the virtual environment. (c) View of the target landmark presented in the bottom left panel. The movements for all participants for the remainder of the execution phase are represented as green lines in the map of the virtual environment. (d) A map of the virtual office landscape, each number indicates the location of one landmark. Most landmarks consisted of several objects as can be seen in panels a and c. Participants could use different pathways but still reach the target successfully.

pads were used to minimize head motion. The fMRI stimuli were presented using MRI compatible LCD goggles with 640×480 resolution (Nordic Neuron Lab, Bergen, Norway). Subjects moved inside the environment using an MRI compatible joystick (Current Designs, Philadelphia, USA).

The participants were first allowed to familiarize themselves with the presentation equipment and joystick. Then the subjects completed four practice trials, one from each experimental condition (see below). Scanning was commenced when complete task compliance was assured.

fMRI paradigm

The fMRI paradigm was jittered, with variable block duration and alternating blocks of navigation (30±2 s) and rest (i.e., fixation; 10± 2 s). There were three navigation conditions and one baseline condition. In all three navigation conditions, participants were placed at a different landmark at the start of each block, and an image of a target landmark was inserted at the bottom center of the screen (Fig. 1). The participants were instructed to navigate towards the target landmark as fast and accurately as possible. All combinations of starting positions and targets were unique to the fMRI experiment and had not been presented during the learning session. The three navigation conditions were condition Normal, Without and Blocked, and the baseline condition was Line following. In condition Normal, the environment was the same as during the learning session, consisting of both borders (i.e., walls) and landmarks. In order to explore the importance of landmarks for successful navigation, condition Without was introduced. In condition Without, all landmarks, except start and target landmarks, were removed. The effect of navigational re-planning when target location was known but blockades directly in front of the target obstructed direct access to it was investigated with condition Blocked. In condition Blocked, all landmarks were in place, but the corridors leading directly to the target landmark were temporally blocked. The blockage, a stop sign, was not visible before the subject came upon it. In all three navigation conditions, the participants were instructed to move as fast and accurately as possible to the target landmark. If the participant reached the landmark before the block ended, a new target landmark was presented. If participants did not find target, they kept on trying until the block was terminated. Block duration was set to 30±2 s. Based on pilot studies, the tasks were designed so that arrival at the first landmark could be achieved well within the time limit of the block, while the second landmark was always beyond range. The baseline condition (Line following) was designed to control for motor and visual components of navigation. Here participants moved in the environment by following a yellow line on the floor. In this condition, all landmarks were removed from the environment, including the start and target landmarks. This was done to prevent subjects from using this condition to learn the environment better, which was found to take place in the pilot studies leading up to the present design. The four navigation and the Line following conditions were separated by 10 s (±2 s) of fixation, which was a white central cross on a black screen. Each participant completed three experimental runs, with five

of each of the four conditions plus 20 fixation blocks in each run. The order of runs was randomized between participants.

Performance data were logged throughout the experiment and extracted with in-house developed software written in Python (Python Software Foundation, Hampton, NH, USA). Success rate was computed as percentage of first target landmarks reached within each block since it was impossible to reach the second target landmark within the given time. Position data of the participants' movements inside the environment were logged with a time interval of 30 ms and can be displayed as a trace (see Fig. 1). Based on the behavioral data obtained from all participants, the speed of the movement and movement paths for all condition Normal trials were estimated and plotted (for example, see Fig. 1).

Imaging parameters

T2*-weighted, blood-oxygen-level-dependent (BOLD) sensitive images were acquired using an echo-planar imaging pulse sequence (TR = 2600 ms, TE = 30 ms, FOV = 244 mm, slice thickness = 3.0 mm, slice number = 47, matrix = 80 × 80 giving an in-plane resolution of 3 × 3 mm). Each functional run contained 327 volumes, with slices positioned as close to 90° on the anterior–posterior direction of the hippocampus as possible. For anatomical reference, one T1-weighted 3D volume was acquired with an MPRage sequence (TR = 2300 ms, TE = 30 ms, FOV = 256 mm, slice thickness = 1.0 mm, matrix 256 × 256, giving an in-plane resolution of 1.0 × 1.0 mm).

Post-scanning

After scanning, the volunteers were given a random sample of tasks performed in the scanner and asked to indicate when the initial phases (self-localization, target localization and path planning) were completed.

Data analysis

Behavioral data

Behavioral data were analyzed in SPSS 14.0 (SPSS Inc., Chicago, Illinois, USA). ANOVA analyses followed by paired *t*-tests for within-subjects comparisons were carried out in order to compare the number of correct answers on the tests of recognition, judgment of direction and judgment of distance and also for comparison of the success rates in condition Normal, Without and Blocked. The distances moved during the initial 4.6 s and the subsequent 4.6 s in condition Normal were compared using a paired *t*-test. Significance level was set to $p<0.05$ for all statistical comparisons. All values are given as Mean ± SD.

MRI data analysis

Imaging data were analyzed using FSL 4.0 (Analysis Group, FMRIB, Oxford, UK). First, non-brain tissue was removed from the T1-weighted anatomical images using BET (Brain Extraction Tool, FMRIB, Oxford, UK), and the resulting images were transformed to the MNI 152 1 × 1 × 1 mm template (Montreal Neurological Institute, Montreal, QC, Canada) with FLIRT (FMRIB, Oxford, UK). The fMRI data were motion corrected using FLIRT, with the median volume of each run as reference. Then each functional run was co-registered to the corresponding anatomical T1 image and transformed into MNI space by using the transformation matrix obtained with the T1 image. The functional data were filtered with a 5-mm full-width at half-maximum Gaussian spatial filter, and a temporal high-pass filter with a cutoff time of 250 s. The statistical analysis of the fMRI data was carried out in FEAT (FEAT, FMRIB, Oxford, UK). Conditions were modeled according to a boxcar stimulus function convolved with a two-gamma hemodynamic response function. The effect of each condition was estimated with GLM using FLAME 1 (FMRIB's local analysis of mixed effects).

A whole brain analysis was performed using first a statistical threshold of $Z \geq 4$ ($p \leq 0.000032$) for each voxel, and then a cluster threshold of $p = 0.05$. The conditions Normal>Line following, Without>Line following and Blocked>Line following and the differences between conditions Normal, Without and Blocked were explored.

Since the region of interest for this study was the medial temporal lobe (MTL), a brain mask was created by combining the probabilistic maps of the Harvard Oxford Structural Atlases and the Juelich Histological Atlas (part of FSL; http://www.fmrib.ox.ac.uk/fsl/fslview/atlas-descriptions.html#ho) (Flitney et al., 2007), using max probability >50% as threshold. In total, the mask encompassed 16 180 1-mm voxels. The entorhinal cortex and the perirhinal cortex were segregated based on anatomical boundaries (Insausti et al., 1998). Contrasts between condition effects were tested for significance using voxel-based thresholding with corrected voxel threshold set to $p<0.05$ and a minimum cluster size of 45 contiguous voxels.

The time courses of the hemodynamic response in condition Normal were calculated for all individuals using PEARL (Pearl event-related time course extraction) 2.61 and each individual's data from FSL (www.jonaskaplan.com/fmritools.html). The percent change in the BOLD signal over time for condition Normal was extracted from a smoothed functional voxel in the anterior and the posterior hippocampus. The anterior voxel was chosen on the basis that it had increased activity in the contrast Initial>Execution phase. The MNI coordinates for this voxel were 25, −20, −18. The posterior voxel was associated with increased activity in the contrast Normal>Line following (whole block analyses), and had MNI coordinates of 29, −35, −14. In addition, the BOLD signal time course plots for unsuccessful versus successful trials in condition Normal were calculated separately for the anterior and posterior voxel.

In order to investigate differences in activation between the initial and the execution phase of the navigation period, each active navigation block was divided into two separate events. Based on the participants' reports, the initial phase (self-localization, target localization and path planning) lasted 4.6 ± 1.2 s (range 3–8 s). The execution phase was the time following the initial phase, lasting until either the first target landmark was reached, or until the block was terminated. In blocks where participants reached the first landmark, a second target landmark was presented, and thus some navigation blocks included two initial phases. A mixed effects FLAME 1 analysis of the contrast initial>execution phase for condition Normal, Without and Blocked was performed in the MTL ROI and on the whole brain level.

Combined fMRI and behavioral data analysis

The subject-specific scores for success rate in condition Normal were added as a separate regressor in the GLM in order to identify regions of activation that correlated with performance across subjects. This was done for activation in condition Normal, for the whole block (Normal>Line following) and for the initial phase (Initial>Execution) using a mixed effects analysis.

Results

Included participants

All 20 subjects were able to complete the structured learning session within the predefined 60-min time limit. However, only 18 individuals were able to complete the fMRI session, and hence only results obtained from these participants are included in the following. The two participants that had to withdraw during scanning experienced severe nausea. Several participants reported nausea but were able to complete scanning. Nausea is common in computer games that involves virtual environments, often referred to as

simulation sickness (Slater et al., 1995), and is supposed to indicate that the participant is properly submerged into the virtual environment.

Tests of knowledge of the virtual environment

The number of correct answers on the recognition test was 9.9 ± 0.3, distance test 9.0 ± 1.0 and direction test 6.3 ± 1.7. The success rates were above chance level in all these tests, indicating that the participants were able to recognize the landmarks, and had a representation of their internal relationship.

fMRI performance and post-scanning assessment of duration of initial phase

In condition Normal, participants were able to reach a 9.0 ± 3.2 of the 15 target landmarks. However, in conditions Without and Blocked, only 5.0 ± 2.5 and 5.2 ± 1.8 landmarks were reached, respectively. The participants failed to reach the target landmark in some of the tasks not because they did not know where the target landmark was located but because they ran out of time. This was verified by the behavioral output. This was particularly noticeable in condition Blocked where all participants were close to the target landmarks but were unable to reach them as there was only one open entry point to the landmark. For the success rate, ANOVA showed a significant effect of condition ($F<0.001$). Post hoc paired comparisons revealed a significant difference both between conditions Normal and Without ($t=5.5$, $p<0.001$) and conditions Normal and Blocked ($t=4.9$, $p<0.001$). Conditions Without and Blocked were not significantly different.

Based on the participants' self-reports when represented with tasks performed during scanning, the initial phase (self-localization, target localization and path planning) lasted 4.6 ± 1.2 s (range 3–8 s). The initial phase was hence set to last 4.6 s for the analyses of the Initial>Execution phase.

Route plot results

The participants moved significantly shorter during the first 4.6 s (3.51 ± 2.91 units of size) compared to the subsequent 4.6 s (10.20 ± 5.39 units of size) ($p<0.001$) in condition Normal. As can be seen in Fig. 1, in the initial phase the subjects mainly remained standing or moved/turned in the vicinity of the start position. During the next 4.6 s, subjects moved towards the target at approximately double speed compared to the initial phase (Fig. 1). These behavioral data corroborate the participants' self-reports, i.e., that the initial phase lasted approximately 4.6 s.

fMRI results

MTL ROI analyses

Activity in the entire navigation blocks for conditions Normal, Without and Blocked. The contrast Normal>Line following gave activations in the posterior part of the right hippocampus, the mid-posterior part of the left hippocampus and bilaterally in parahippocampal cortex (Fig. 2; Table 1). The contrasts Blocked>Line following and Without>Line following gave activations in the parahippocampal cortex, bilaterally (Fig. 2; Table 1).

The contrasts Normal>Without showed significantly increased activity in the left posterior hippocampus, whereas Normal>Blocked had significantly increased activity in the right anterior and posterior hippocampus plus the left posterior hippocampus. Also the parahippocampal cortex had increased activity bilaterally in Normal>Blocked (Table 2). The left and right anterior hippocampi were significantly more active in condition Without>Blocked. The contrasts Blocked>Normal and Without>Normal showed no increase in activation.

Initial versus Execution phase for conditions Normal, Without and Blocked. For conditions Normal and Blocked, a comparison of the initial phase with the execution phase yielded activation in bilateral anterior and posterior hippocampus, rostral and caudal right entorhinal cortex and right anterior parahippocampal cortex (Fig. 3; Table 3). For condition Blocked, activation was also observed in the caudal part of the left entorhinal cortex and in the left perirhinal cortex. The same comparison for condition Without revealed activation in the posterior right hippocampus, the anterior and posterior left hippocampus, the caudal part of the right entorhinal cortex and the left parahippocampal cortex. No significant differences were found when comparing the initial phases between conditions indicating that the initial phases recruited similar regions independent of upcoming navigational demands.

Comparison of execution phases for conditions Normal, Without and Blocked. In the execution phase in the contrast Normal>Without, increased activations were observed bilaterally in the hippocampus and in the right parahippocampal cortex. In the contrast between the execution phases for condition Normal>Blocked increased activations in bilateral hippocampi and parahippocampal cortices were observed. There were no significant activations when contrasting the execution phases for Without>Normal and Blocked>Normal.

Activity correlated with performance for condition Normal. In condition Normal>Line following, there was a positive correlation with activity in the right anterior hippocampus and left parahippocampal cortex and success rate (Fig. 4; Table 4). For the initial phase of navigation (Initial>Execution), activation in the anterior right hippocampus showed a significant correlation with performance (Fig. 4; Table 4).

Whole brain analyses

Conditions Normal, Without and Blocked versus Line following. Contrasts Normal>Line following, Blocked>Line following and Without>Line following all revealed increased activation bilateral in the occipital cortex, anterior insula, precuneus, fusiform gyrus and parahippocampal cortex and in the right lateral prefrontal cortex and thalamus (Fig. 5; Table 5). In both hemispheres, the precuneus and fusiform gyrus activations were interconnected and spread anteriorly into posterior cingulate cortex and inferiorly into lingual gyrus in both hemispheres. Activation in the right hippocampus was only observed for contrast Normal>Line following at the whole brain level.

Differences between conditions Normal, Without and Blocked. In the contrast Normal>Without, increased activation was found in bilateral lateral occipital cortex, spreading inferomedially into the fusiform gyri (Table 6). The contrast Normal<Without showed no regions with increased activity. Normal>Blocked had increased activation bilaterally in lateral occipital cortices and hippocampi. In both hemispheres, the parieto-occipital activations spread into the entire hippocampus. In Normal<Blocked, increased activations were present in bilateral superior medial prefrontal cortex, left dorsolateral and right inferior prefrontal cortex (Table 6). There was also increased activity in bilateral angular gyrus and right middle temporal gyrus. In Without>Blocked, increased activation was found in the right hippocampus. Condition Without<Blocked had increased activation in the bilateral cingulate cortex spreading into the precuneus, right medial superior frontal gyrus and left dorsolateral prefrontal cortex. There was also increased bilateral supramarginal gyrus activity spreading inferiorly and increased activity in the right superior temporal gyrus (Table 6).

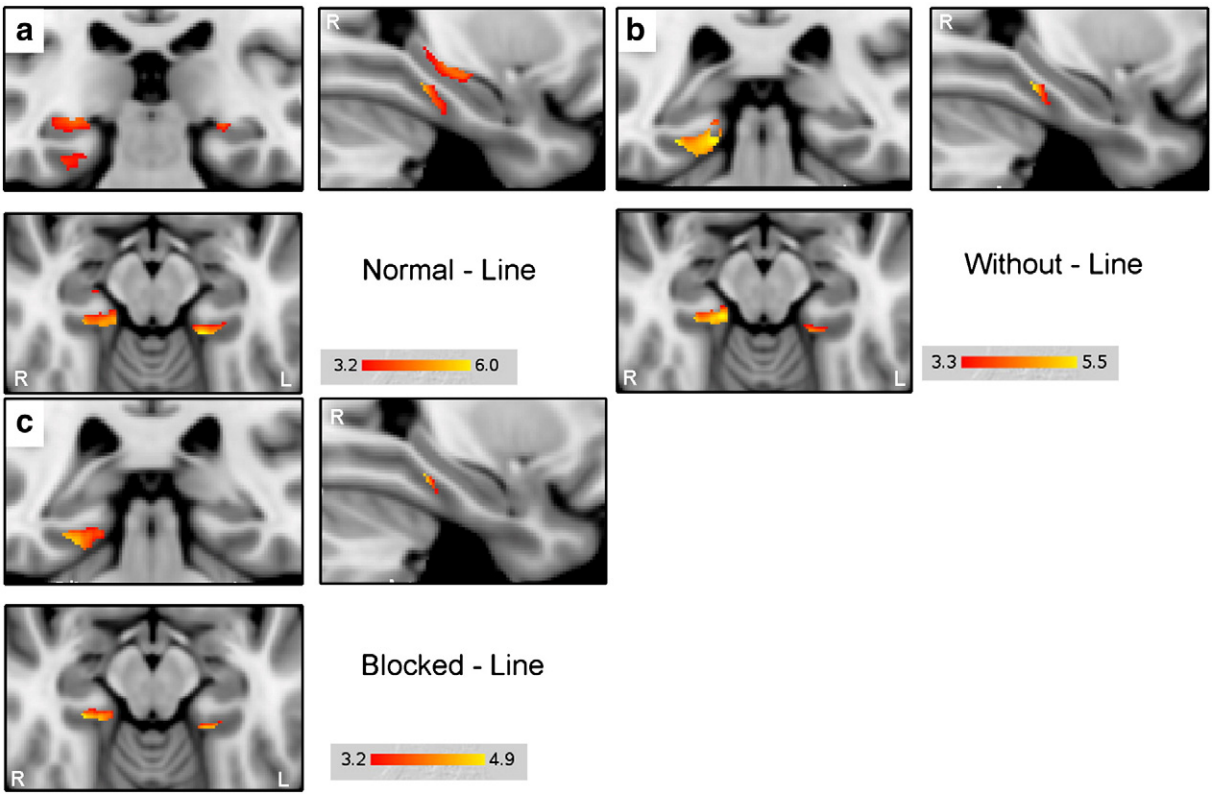

Fig. 2. Medial temporal lobe (MTL) regions with increased activity for the entire navigation block compared with the baseline condition Line following. (a) Condition Normal>Line following; (b) condition Without>Line following; (c) condition Blocked>Line following. The analysis was carried out using a hippocampal–parahippocampal gyrus mask and voxel-based thresholding, $p<0.05$ corrected. Minimum cluster size was 45 voxels. Activations are superimposed on the MNI, Montreal Neurological Institute 152 brain template. Left is right in the figure.

Initial versus execution phase for condition Normal. When comparing the initial phase and the rest of the way-finding block in condition Normal, increased activations were observed in both hippocampi, anterior and posterior cingulate gyrus, precuneus, middle temporal gyrus, fusiform gyri, caudate nuclei, occipital cortices and thalamus (Fig. 6; Table 7).

Time course analyses. In the smoothed functional voxel in the right anterior hippocampus (upper panel, Fig. 7), the BOLD signal increased initially and then decreased before it increased again at the end of condition Normal (Fig. 7). The second increase in the BOLD signal coincides with the participants reaching the first target and getting the second navigation task in condition Normal. The BOLD signal in the anterior hippocampus voxel was higher for the initial phases when navigation was successful than when navigation was unsuccessful (middle panel, Fig. 7). In the smoothed functional voxel in the posterior hippocampus, the BOLD signal fluctuated throughout condition Normal, independent of navigational phases and there was no apparent difference in BOLD signal and successful versus unsuccessful navigation (lower panel Fig. 7).

Table 1
Regions within the medial temporal lobe (MTL) with increased activity in the conditions Normal, Without and Blocked versus the baseline condition (Line following).

MTL region	Coordinates of peak activation (MNI)			Cluster size (no. of voxels)	*Z*-score
	X	*Y*	*Z*		
Normal>Line following					
R. Hippocampus	29	−35	−14	567	5.19
L. Hippocampus	−23	−29	−8	58	4.73
R. Parahippocampal cortex	29	−35	−14	632	5.19
L. Parahippocampal cortex	−21	−41	−13	209	6.00
Without>Line following					
R. Parahippocampal cortex	17	−34	−15	557	5.57
L. Parahippocampal cortex	−21	−41	−13	69	4.66
Blocked>Line following					
R. Parahippocampal cortex	28	−36	−14	305	4.83
L. Parahippocampal cortex	−21	−41	−13	53	4.94

The analysis was carried out using a hippocampal–parahippocampal gyrus mask and voxel-based thresholding, $p=0.05$ corrected for multiple comparisons. MNI, Montreal Neurological Institute 152 brain template, has voxel resolution of 1 mm^3. Only clusters with a cluster size >45 voxels were reported. R; right; L, left.

Table 2
Peak activations in the medial temporal lobe (MTL) ROI when comparing the conditions Normal, Without and Blocked.

MTL region	Coordinates of peak activation (MNI)			Cluster size (no. of voxels)	*Z*-score
	X	Y	Z		
Normal>Without					
L. Hippocampus	−21	−31	−7	102	4.25
Without>Normal (no significant increase in activation observed)					
Normal>Blocked					
R. Hippocampus	30	−39	0	102	5.33
	35	−18	−21	68	4.25
L. Hippocampus	−31	−38	−5	312	5.12
L. Parahippocampal cortex	−27	−32	−21	83	4.45
Blocked>Normal (no significant increase in activation observed)					
Without>Blocked (no significant increase in activation observed)					
Blocked>Without (no significant increase in activation observed)					

The analysis was carried out using a hippocampal–parahippocampal gyrus mask, i.e., an MTL ROI, and voxel-based thresholding, $p=0.05$, corrected for multiple comparisons. MNI, Montreal Neurological Institute 152 brain template, has voxel resolution of 1 mm^3. Only clusters with a cluster size >45 voxels were reported. R, right; L, left.

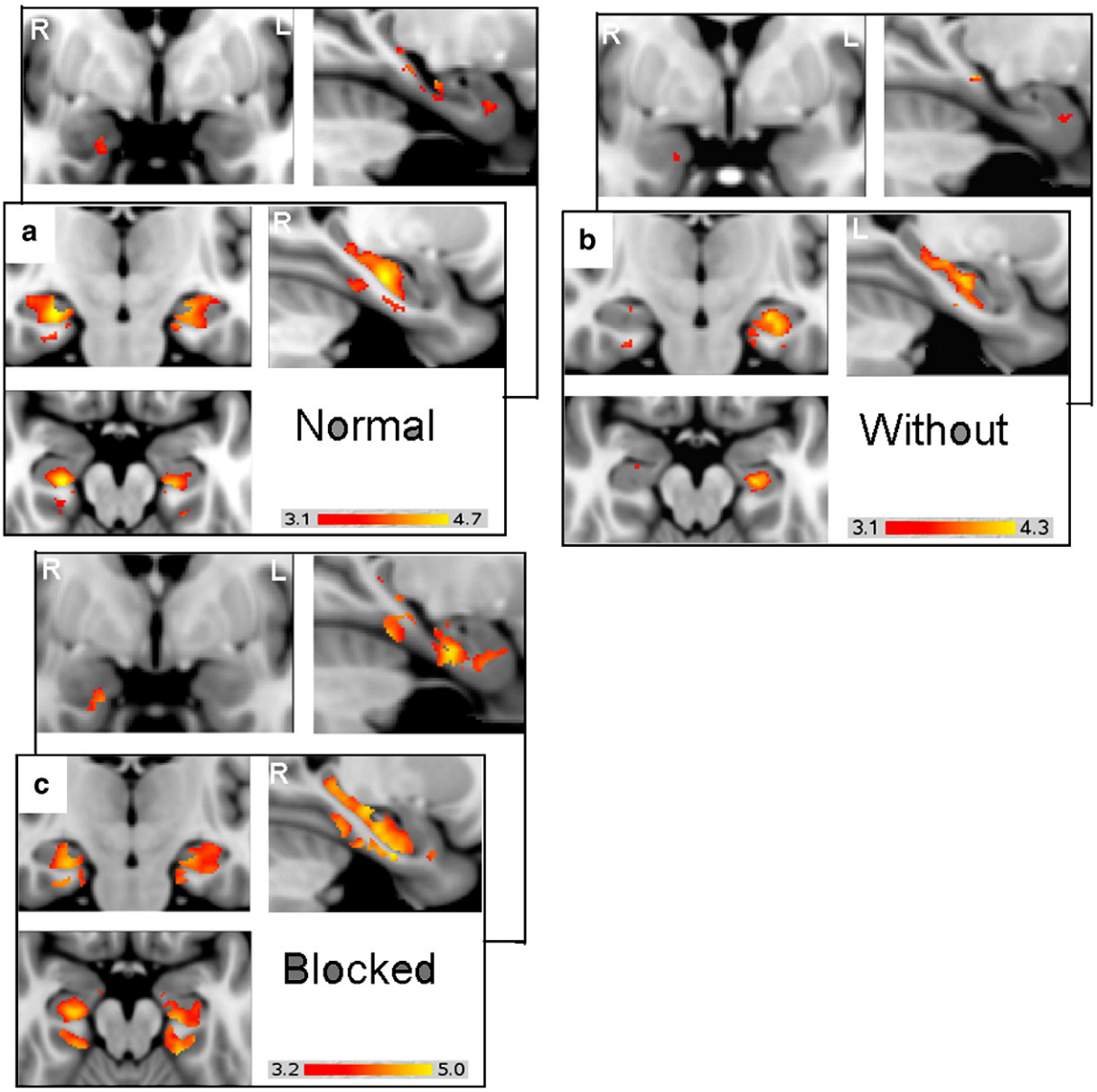

Fig. 3. Medial temporal lobe (MTL) regions with increased activity in the initial phase compared to the execution phase of the navigation block. (a) Condition Normal; (b) condition Without; and (c) condition Blocked. The analysis was carried out using a hippocampal–parahippocampal gyrus mask and voxel-based thresholding, $p<0.05$ corrected for multiple comparisons. Minimum cluster size was 45 voxels. Activations are superimposed on the MNI, Montreal Neurological Institute 152 brain template. Left is right in the figure.

Discussion

The aim of the present study was to compare activation of MTL subregions in the initial phase and execution phase of navigation, measured during different navigational demands. The main finding is a functional segregation within the MTL with regard to navigational phase. In the initial phase of navigation, there was increased activation of the anterior MTL, i.e., the anterior hippocampus, entorhinal cortex and anterior parahippocampal cortex, whereas activity in the posterior MTL, i.e., posterior hippocampus and posterior parahippocampal cortex, was present throughout navigation. An additional finding was that the posterior hippocampal activity depended on both environmental features and navigational demands, i.e., presence or absence of landmarks and blockades.

The finding of increased anterior MTL activity in the initial phase suggests that this region is specifically engaged in self-localization, target localization and/or path planning. The posterior MTL, on the other hand, appears to be involved in processing input from the current location, i.e., representing information necessary for recognition and/or recall. To our knowledge, this study is also the first human imaging study to detect entorhinal activation in a direct comparison between specific navigational conditions, substantiating that the human entorhinal cortex, like the rodent entorhinal cortex, is active during spatial navigation.

The duration of the initial phase of navigation was determined based on the participants' self-reports following scanning and gave a crude estimate of the amount of time required for self-localization, target localization and planning. The self-reported duration of the initial phase concurred with the behavioral changes observed in the participants' movement plots and the significant increase in their speed of movement after the initial 4.6 s. The BOLD signal time course plots in the anterior hippocampus associated with the initial phase similarly showed a transient initial increase lasting approximately five seconds. This finding corroborates the self-reports and the movement data. Unfortunately, an option for more direct measures of self-localization, target localization and path planning was unavailable.

Table 3
Peak activations within the medial temporal lobe (MTL) ROI when comparing Initial phase>Execution phase in conditions Normal, Without and Blocked.

MTL region	Coordinates of peak activation (MNI)			Cluster no.	Cluster size (no. of voxels)	Z-score
	X	Y	Z			
Normal						
R. Hippocampus	25	−20	−18	1	1223	4.80
	23	−25	−11	*(1)*		4.37
	24	−32	−8	*(1)*		3.89
	31	−17	−14	*(1)*		3.77
L. Hippocampus	−22	−23	−15	2	1311	4.49
	−20	−16	−15	*(2)*		3.90
	−20	−30	−10	*(2)*		3.82
R. Entorhinal cortex	20	−2	−23	3	45	3.65
	25	−19	−25	*(1)*		3.66
R. Parahippocampal cortex	28	−29	−23	4	116	3.73
L. Parahippocampal cortex	−15	−32	−10	5	49	4.16
	−29	−35	−15	6	198	4.00
Without						
R. Hippocampus	20	−31	−6	1	69	3.91
L. Hippocampus	−20	−34	−5	2	1042	4.37
	−27	−17	−20	(2)		4.12
	−24	−25	−11	(2)		3.94
R. Entorhinal cortex	27	−17	−28	3	56	3.46
Blocked						
R. Hippocampus	26	−22	−12	*(1)*		5.00
	26	−12	−27	*(1)*		4.83
	23	−35	−3	*(1)*		4.53
L. Hippocampus	−19	−34	−7	4	2395	4.64
	−22	−24	−16	*(4)*		4.36
	−20	−17	−18	*(4)*		4.12
R. Entorhinal cortex	26	−13	−29	1	2930	5.00
	19	−3	−27	*(1)*		4.13
L. Entorhinal cortex	−17	−17	−27	*(4)*		4.10
L. Perirhinal cortex	−30	−7	−32	2	62	3.92
R. Parahippocampal cortex	21	−35	−18	3	759	4.51
	26	−24	−25	*(3)*		4.47
L. Parahippocampal cortex	−15	−32	−10	4	3535	5.01
	−24	−40	−14	*(4)*		4.73
	−24	−23	−25	*(4)*		4.24

The analysis was carried out using a hippocampal–parahippocampal gyrus mask and voxel-based thresholding, $p = 0.05$ corrected for multiple comparisons. MNI, Montreal Neurological Institute 152 brain template, has voxel resolution of 1 mm^3. The cluster number is given in parenthesis for secondary peaks within the respective clusters. Numbers in the cluster size column represent the actual number of voxels within the anatomical region in the respective row. R, right; L, left.

Table 4
Peak activations within the medial temporal lobe (MTL) ROI correlating with success rate in condition Normal for the whole block and for the Initial>Execution phase.

MTL region	Coordinates of peak activation (MNI)			Cluster No.	Cluster size (no. of voxels)	Z-score
	X	Y	Z			
Whole block						
R. Hippocampus	23	−38	4	1	70	2.43
	26	−20	−16	2	89	2.25
L. Parahippocampal cortex	−24	−34	−19	3	60	2.00
Initial>Execution phase						
R. Hippocampus	27	−10	−28	1	47	2.24

The analysis was carried out using a hippocampal–parahippocampal gyrus mask and voxel-based thresholding, $p = 0.05$ uncorrected. MNI, Montreal Neurological Institute 152 brain template, has voxel resolution of 1 mm^3. Only clusters with a cluster size >45 voxels were reported. R, right; L, left.

Such an approach would have been ideal to explore each component separately and also to take into account differences between subjects and between the different tasks.

In the initial phase of navigation, increased activity was detected in both the rostral and caudal entorhinal cortex. This was similar across all navigational conditions. In previous neuroimaging studies of spatial navigation, only a few have reported activation in the entorhinal cortex (Doeller et al., 2010; Spiers and Maguire, 2007a).

The initial increase in the caudal entorhinal activity can reflect processing of landmarks and perhaps more specifically their spatial arrangement. Several neuroimaging studies of spatial memory have reported activation in the caudal entorhinal cortex during recognition and retrieval of object locations as well as during spatial ordering of objects (Adcock et al., 2006; Johnsrude et al., 1999; Owen et al., 1996). Moreover, visually responsive cells in the caudal entorhinal cortex in monkeys respond to particular objects or places (Owen et al., 1996; Suzuki et al., 1997). In addition to engendering object–place associations, grid cells in the caudal entorhinal cortex may provide a representation of self-localization within an environment together with the hippocampal place cells (Doeller et al., 2010; Fyhn et al., 2004; Moser et al., 2008). It is possible that the increased activity in the initial phase of the navigation block reflects a transient re-setting of the entorhinal grid cell activity when the subjects enters at a new location at the beginning of each trial. In rats, it has recently been shown that grid cell representations are discontinuous within an environment divided by geometric boundaries (Derdikman et al., 2009). The rostral entorhinal activity detected in the initial phase is equivalent to activity observed during retrieval of stored associations (Kirwan and Stark, 2004; Tyler et al., 2004) and in response to objects presented in the same order as previously experienced in a virtual environment (Janzen and Weststeijn, 2007). It can be speculated that the complex landmarks used in this virtual environment may have particularly engaged the rostral entorhinal cortex since they were made up of combinations of objects rich in non-spatial content as compared to the more simplistic and/or solitary landmarks used in most other virtual navigation studies (Antonova et al., 2009; Doeller et al., 2008; Ekstrom and Bookheimer, 2007; Iaria et al., 2007; Parslow et al., 2005; Peigneux et al., 2004; Rauchs et al., 2008; Shipman and Astur, 2008).

The virtual environment used in the present experiment was large compared to those used in most neuroimaging studies of navigation (Antonova et al., 2009; Doeller et al., 2008; Ekstrom and Bookheimer, 2007; Grön et al., 2000; Iaria et al., 2007, 2008; Jordan et al., 2004;

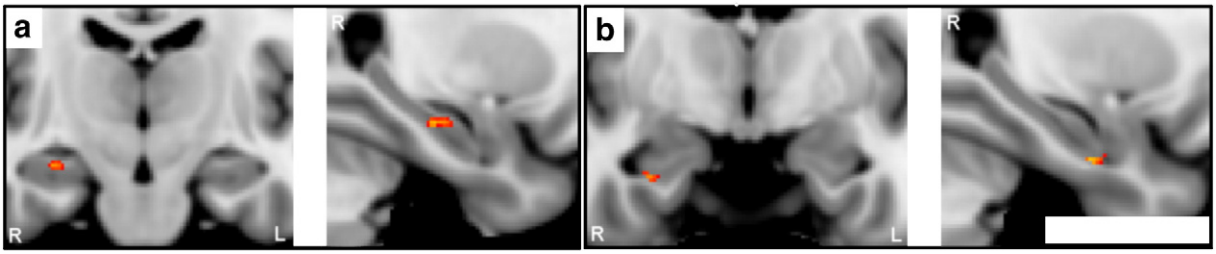

Fig. 4. Correlation between activation and the navigation success in condition Normal. (a) Whole block activity for condition Normal>Line following and (b) Initial>Execution phase in condition Normal. The analysis was carried out using a hippocampal–parahippocampal gyrus mask and voxel-based thresholding, $p<0.05$ uncorrected. Minimum clusters cluster size was 45 voxels. Activations are superimposed on the MNI, Montreal Neurological Institute 152 brain template. Left is right in the figure.

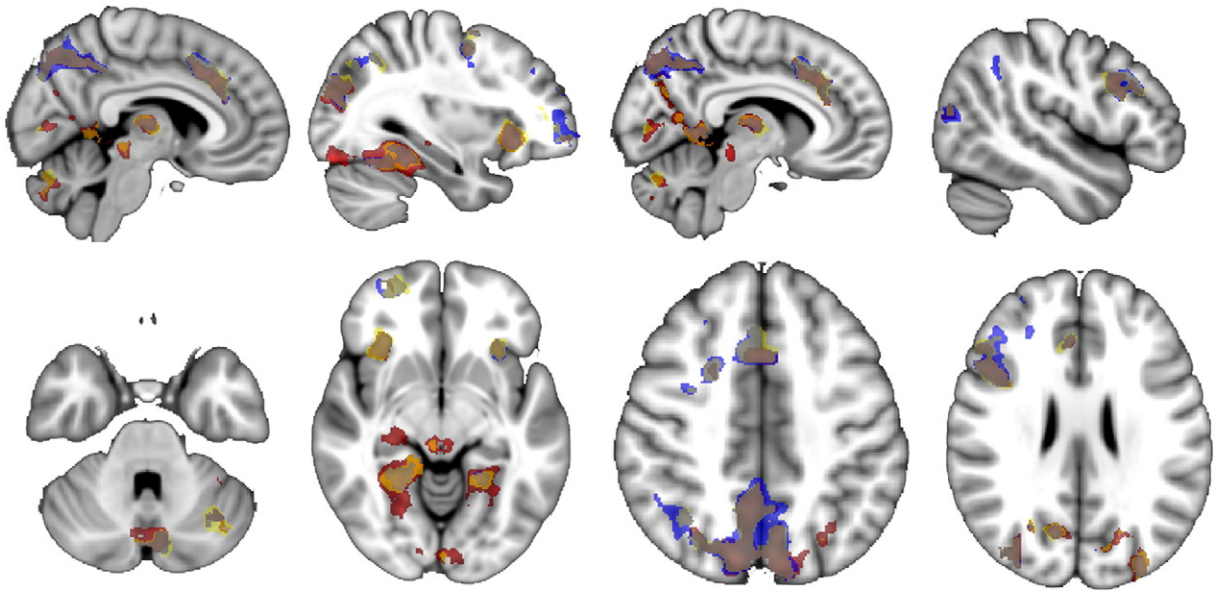

Fig. 5. Statistical parametric maps of increased brain activity for the different navigational conditions superimposed on top of each other on the MNI, Montreal Neurological Institute, 152 template brain. Condition Normal>Line following in red, condition Without>Line following in blue and condition Blocked>Line following in yellow. Voxel-based thresholding, $p<0.05$ corrected for multiple comparisons, was applied. Right hemisphere is on the left in the figure.

Ohnishi et al., 2006; Parslow et al., 2005; Peigneux et al., 2004; Rauchs et al., 2008; Shipman and Astur, 2008). The size of the virtual environment to be mentally represented may be an important determinant for increasing the entorhinal activity. Supporting this notion is the positive correlation between entorhinal activity and increasing distance to target (Spiers and Maguire, 2007a). Based on previous behavioral studies (Spiers and Maguire, 2008), subjects appear to engender a more global representation of the entire virtual environment in order to determine target location and choose the appropriate path. When executing the navigational plan, a limited representation of the virtual environment may suffice, possibly leading to a decline in entorhinal activity. Indeed, spatial reference memory has been shown not to be updated during locomotion in humans (Mou et al., 2004), and one human lesion study demonstrates that entorhinal cortex is not necessary for path integration (Shrager et al., 2008).

Lack of entorhinal activation in many fMRI studies of navigation studies could be due to susceptibility artifacts in T2*-weighted BOLD fMRI. These artifacts are most pronounced in the entorhinal cortex (Ojemann et al., 1997). The slice orientation in the present study reduces this problem (Chen et al., 2003). The presence of such susceptibility artifacts in BOLD fMRI may explain why PET studies have detected entorhinal activity in mental navigation (Ghaem et al., 1997; Mellet et al., 2000), which has not been reproduced in comparable fMRI studies (Avila et al., 2006; Kumaran and Maguire, 2005). It should be noted that brain activity detected using fMRI only depicts differences in activity in one condition relative to another. Persistent entorhinal cortex activity across all conditions can therefore not be visualized. Still, our results clearly demonstrate a dynamic role for the entorhinal cortex, with increased engagement in the initial phase of navigation.

The initial phase of navigation was also associated with increased activation in the anterior hippocampus. This activation may reflect a type of mental navigation and also as a type of self-projection or prospection, i.e., looking into the future. This is supported by behavioral data demonstrating that individuals use mental imagery as strategy for navigational planning (Spiers and Maguire, 2008). Also consistent with this interpretation, bilateral anterior hippocampal activity has been found in self-projection (Addis et al., 2009; Szpunar et al., 2007), and the location of this activity is similar to the bilateral anterior hippocampal activity detected in the initial phase in the present navigation study. Equivalent anterior hippocampal activity has also been reported in studies of mental navigation (Ghaem et al., 1997; Mellet et al., 2000), bird's eye view navigation (Jordan et al., 2004) and during navigational planning (Spiers and Maguire, 2006). Mental and bird's eye view navigation entail entering an imaginary, non-actual view of one's position and actions in space. Changing one's point of view from first to third person's perspective also correlates with bilateral anterior hippocampal activity (Schmidt et al., 2007). The bilateral anterior hippocampal activity in the initial phase of navigation thus seems to draw on similar regions in the MTL as mental imagery, prospection and third person's point of view (Addis et al., 2009; Szpunar et al., 2007). This suggests that self-localization, target localization and path planning involve construction of a mental representation of the environment based on a meta-perspective of the layout. Furthermore, in rats the hippocampus is also involved in planning of future actions, i.e., vicarious trial and error (Hu and Amsel, 1995), which is considered the rodent equivalent of self-projection.

Right anterior hippocampal activity similar to that in the initial phase of navigation has also been associated with target localization (Doeller et al., 2008; Schmidt et al., 2007; Shipman and Astur, 2008), especially when there is increasing demands on memory-based navigation (Shipman and Astur, 2008), as well as with navigational planning and re-planning (Spiers and Maguire, 2006). The finding that navigational success in condition Normal correlated with activation in the right anterior hippocampus for the initial phase demonstrates an important role for the anterior hippocampus in accurate navigation. Indeed, time course plots of the BOLD signal in the functional voxel in the anterior hippocampus clearly showed that unsuccessful trials had no increase in the BOLD signal while successful did. Activity in this voxel hence predicted the subject's success 15 to 20 s later. Previously, path integration (Wolbers et al., 2007) and spatial coding (Schmidt et al., 2007) have been shown to correlate with activity in similar locations in the right anterior hippocampus as in the current study. The anterior hippocampus is considered to support relational processing (Kirwan and Stark, 2004; Schacter and Wagner, 1999), including flexible (re)combination of elements extracted from previous learned associations (Preston et al., 2004), and may therefore be ideally suited to build a mental model based on previous experiences in the virtual environment. This is corroborated

Table 5
Peak activations for the whole brain analyses when comparing the conditions Normal, Without and Blocked, with the baseline condition (Line following).

Brain region	Coordinates of peak activation (MNI)			Z-score
	X	Y	Z	
Normal>Line following				
R. Frontal pole	29	55	−5	4.78
R. Superior frontal gyrus	25	8	54	5.02
R. Inferior frontal gyrus	47	13	30	5.11
L. Medial frontal gyrus	0	13	46	6.47
R. Insular cortex	33	22	−6	5.53
L. Insular cortex	−30	23	−2	5.17
R. Precuneus	14	−59	15	6.43
L. Lingual gyrus	−21	−43	−14	6.53
R. Occipital cortex	25	−49	−10	6.92
	33	−80	17	5.30
L. Occipital cortex	−32	−86	23	6.61
L. Fusiform gyrus	−24	−45	−15	6.56
R. Hippocampus	26	−22	−11	4.86
R. Thalamus	7	−17	9	5.75
L. Thalamus	−7	−17	9	5.57
Without>Line following				
R. Frontal pole	26	57	−8	5.30
	28	38	31	4.93
	28	55	21	4.72
R. Superior frontal gyrus	26	7	53	5.75
R. Middle frontal gyrus	28	38	31	4.93
R. Inferior frontal gyrus	48	12	29	5.61
R. Medial frontal gyrus	5	32	31	6.45
R. Insular cortex	32	22	−3	6.09
	41	−79	18	5.13
L. Insular cortex	−31	24	−2	5.36
R. Precuneus	12	−77	43	6.11
L. Precuneus	−3	−67	54	5.99
R. Lingual gyrus	8	−49	−1	5.89
L. Lingual gyrus	−21	−45	−14	5.90
R. Occipital cortex	26	−49	−10	6.37
L. Occipital cortex	−32	−86	24	6.65
L. Fusiform gyrus	−35	−76	−22	
R. Thalamus	7	−19	9	5.32
Blocked>Line following				
R. Frontal pole	30	57	−5	5.47
R. Middle frontal gyrus	49	21	34	5.31
R. Orbitofrontal cortex	32	24	−6	5.38
L. Orbitofrontal cortex	−30	24	−7	5.29
R.&L. Precuneus	0	12	47	6.30
R. Precuneus	12	−77	43	6.47
L. Precuneus	−3	−67	54	6.14
L. Lingual gyrus	−9	−52	−1	5.02
R. Occipital cortex	34	−84	30	5.43
L. Occipital cortex	−31	−83	22	5.33
	−32	−62	39	4.77
	−24	−45	−15	5.79
L. Fusiform gyrus	−36	−74	−21	5.90
R. Thalamus	8	−13	7	4.85

Whole brain analysis was carried out using first a voxel threshold ($Z \geq 4$), and then a cluster threshold ($p = 0.05$, corrected for multiple comparisons). MNI, Montreal Neurological Institute 152 brain template, has voxel resolution of 1 mm^3. Only clusters with a cluster size >45 voxels were reported. R, right; L, left.

Table 6
Peak activations in the whole brain analyses comparing the conditions Normal, Without and Blocked.

Brain region	Coordinates of peak activation (MNI)			Z-score
	X	Y	Z	
Normal>Without				
R. Lateral occipital cortex	30	−94	−12	6.05
L. Lateral occipital cortex	−30	−94	−11	5.91
Without>Normal (no significant increase in activation observed)				
Normal>Blocked				
R. Lateral occipital cortex	25	−97	−12	5.38
L. Lateral occipital cortex	−21	−94	−10	5.45
R. Parieto-occipital sulcus[a]	34	−41	−2	5.45
L. Parieto-occipital sulcus[a]	−28	−41	1	5.13
Blocked>Normal				
R. Superior frontal gyrus	13	51	30	5.70
L. Superior frontal gyrus	−19	57	26	4.95
R. Middle temporal gyrus	59	−57	−5	5.08
L. Middle frontal gyrus	−39	18	40	5.06
R. Inferior frontal gyrus	48	46	−14	5.19
R. Angular gyrus	54	−41	39	5.69
L. Angular gyrus	−55	−52	36	5.26
Without>Block				
R. Hippocampus	31	−40	1	4.65
Blocked>Without				
R. Middle frontal gyrus	34	27	43	4.84
R. Supramarginal gyrus	58	−42	19	5.08
L. Medial superior frontal gyrus	5	48	25	4.81
L. Supramarginal gyrus	−58	−44	34	4.46
R. Cingulate sulcus	0	−17	46	4.64
R. Precuneus	3	−54	63	5.24

Whole brain analysis was carried out using first a voxel threshold ($Z \geq 4$) and then a cluster threshold ($p = 0.05$, corrected for multiple comparisons). MNI, Montreal Neurological Institute 152 brain template, has voxel resolution of 1 mm^3. Only clusters with a cluster size >45 voxels were reported. R, right; L, left.

[a] Cluster includes activation in the hippocampus.

by animal studies where the anterior hippocampus has been shown to support a unitary representation of the environment at large (Kjelstrup et al., 2008). All together, these findings suggest that successful initial retrieval and/or re-encoding of the environment at large in the anterior hippocampus is required in order to find the target. Another possibility is that the anterior part of the hippocampus supports more non-spatial aspects (Jung et al., 1994; Royer et al., 2010), for example, associating information into a coherent plan.

In condition Normal, hippocampal activity was observed throughout the entire navigational period. The center of gravity for this enduring activity was in the right posterior hippocampus, similar to

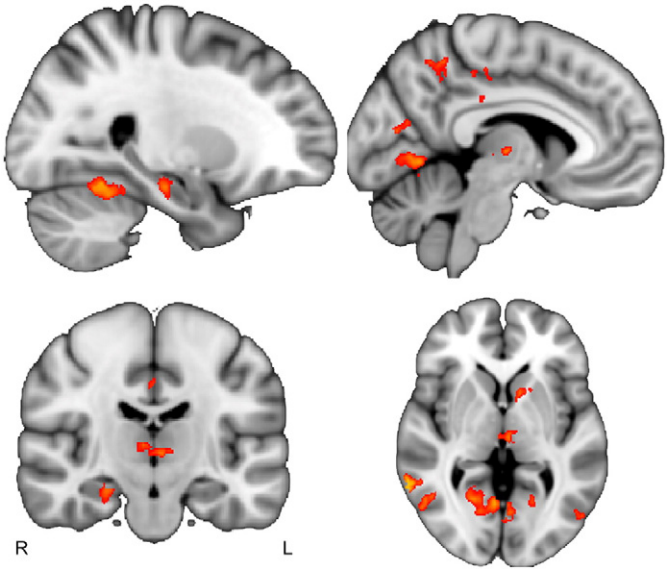

Fig. 6. Comparison between the initial phase and the execution phase for condition Normal on the whole brain level presented on the MNI, Montreal Neurological Institute 152 template, brain. The thresholding was voxel based, $p<0.05$, corrected for multiple comparisons. Right hemisphere is on the left in the figure.

Table 7
Peak activations for whole brain analyses comparing the contrast Initial>Execution phase in condition Normal.

Brain region	Coordinates of peak activation (MNI)			*Z*-score
	X	*Y*	*Z*	
R. Cingulate gyrus, anterior part	2	−11	41	4.71
R. Cingulate gyrus, posterior part	1	−38	29	4.42
L. Cingulate gyrus, posterior part	−12	−38	38	4.94
L. Postcentral gyrus	−37	−36	57	5.19
R. Middle temporal gyrus	62	−52	3	5.30
	52	−61	0	5.09
L. Precuneus	−6	−50	52	4.49
L. Lateral occipital cortex	−51	−63	7	5.18
R. Cuneal cortex	2	−83	22	5.09
L. Primary visual cortex	−7	−76	14	4.52
L. Lingual gyrus	−17	−64	−4	5.27
R. Hippocampus	25	−20	−18	4.80
L. Caudate nucleus	−11	10	0	4.64
L. Thalamus	−4	−17	2	4.71
L. Cerebellum	−36	−50	−26	5.37

Whole brain analysis was carried out using first a voxel threshold ($Z \geq 4$), and then a cluster threshold, $p = 0.05$, corrected for multiple comparisons. MNI, Montreal Neurological Institute 152 brain template, has voxel resolution of 1 mm^3. Only clusters with a cluster size >45 voxels were reported. R, right; L, left.

that observed in numerous fMRI studies of way finding in familiar virtual towns or indoor environments (Antonova et al., 2009; Iaria et al., 2007; Peigneux et al., 2004; Rauchs et al., 2008). A time course analysis of the BOLD signal revealed that this posterior hippocampal activation peaked regularly throughout the navigation epoch. Using multivariate pattern analysis, a recent study demonstrated that accurate allocentric differentiation of position within a familiar environment is located to the right hippocampus (Hassabis et al., 2009), with coordinates similar to those observed in condition Normal for the entire navigation block in this study. This may be taken to suggest that the posterior hippocampal activity represents environmental detail, supporting theories based on rodent models (Moser and Moser, 1998). The fact that posterior hippocampal activity was observed only in condition Normal indicates that a familiar, stable environment is important to produce positional activity within the hippocampus. This posterior hippocampal activity could be related to both retrieval and re-encoding (Giovanello et al., 2009). When the environment was changed by removing landmarks or blocking paths, posterior hippocampal activity was not observed.

The differences observed in MTL activation between the different way-finding conditions are not merely reflecting differences in performance but are related to task demands. Performance was similar in conditions Blocked and Without, and still the contrast Without>Blocked yielded increased hippocampal activation. However, performance measured as success rate is biased, as shown by the movement plots. Subjects were always close to the targets in

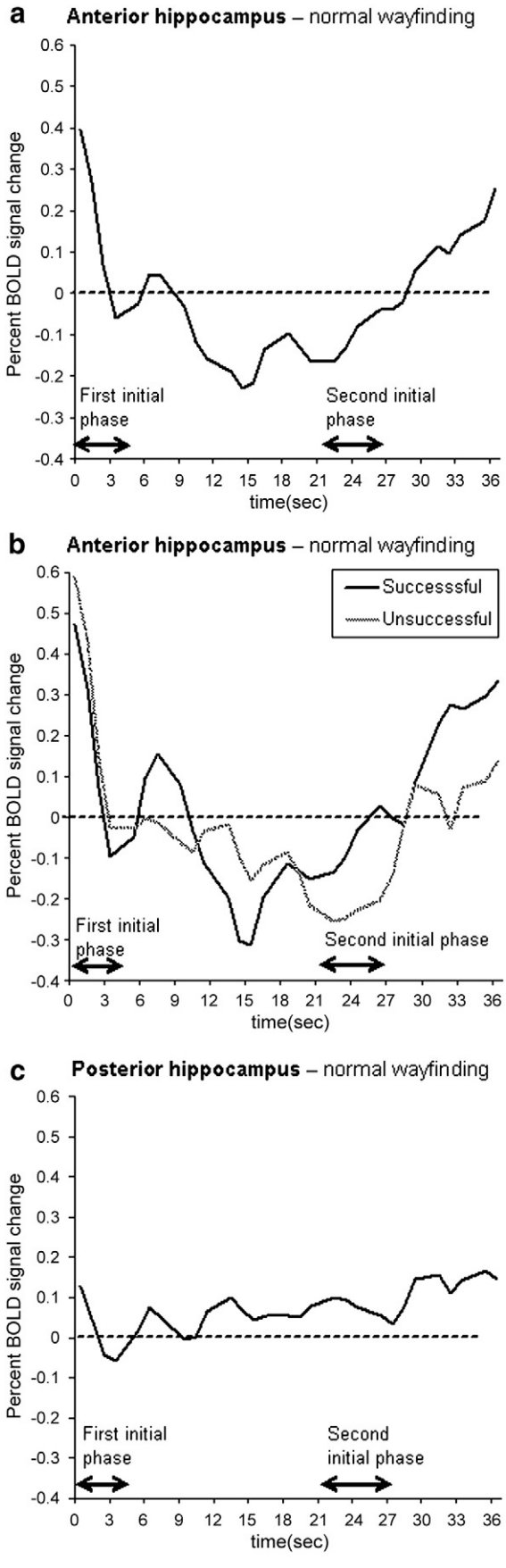

Fig. 7. Plots of the BOLD signal time course changes (% of baseline) in the hippocampus during condition Normal. The baseline signal was the average BOLD signal for all conditions in each run. (a and b) BOLD signal changes in a smoothed functional voxel in the anterior hippocampus. The voxel used in the analysis was the voxel with peak activity in the contrast initial>execution phase in condition Normal (25, −20, −18). (b) BOLD signal changes in the same smoothed functional voxel in the anterior hippocampus. Activity in the voxel in successful (black line) and unsuccessful (gray line) trials are shown. (c) BOLD signal changes in a smoothed functional voxel in the mid-posterior part of the hippocampus. The voxel used in the analysis was the voxel with peak activity in condition Normal for the entire navigation phase>Line following (baseline condition). The voxel coordinates were 29, −35, −14. The BOLD signal time course plots were similar in the posterior hippocampus in successful and unsuccessful trials, results not shown. The BOLD signal related to the initial phases appears delayed due to the lag in the BOLD response with regard to the onset of neuronal activity. The duration of the initial phase was defined based on the participants' post-scan self-reports to last 4.6 s, which was corroborated by the behavioral movement data (see Fig. 1 and Results for details).

condition Blocked, but not in condition Without, still the success rate was similar.

As noted above, condition Blocked did not have persistent hippocampal activity during navigation. The execution phase in condition Blocked resembles to some extent the Morris water maze (Morris, 1984) with visible platform since targets were visible quite early in the navigation block. It has been shown in humans that navigation under conditions similar to this does not require hippocampal activity (Shipman and Astur, 2008). An alternative interpretation is suppression of MTL activity by the rostral medial prefrontal cortex (Anderson et al., 2004; Miller and Cohen, 2003; Spiers and Maguire, 2006). The medial rostral prefrontal cortex was significantly more active during condition Blocked and accompanied by reduced MTL activity. Indeed, condition Blocked had even lower hippocampal activity than condition Without activity as clearly demonstrated in the contrast Without>Blocked. Thus, having actually seen the target but been unable to reach it led to reduced MTL activity and increased prefrontal activity.

In the current study, the anterior parahippocampal cortex was more active in the initial phase, whereas the posterior part was active throughout the navigational period in all conditions. In other words, the parahippocampal cortex displayed an anterior–posterior division of activity during the course of navigation, similar to the hippocampus. It should be noted that current evidence for functional segregation within the parahippocampal cortex is limited, and the interpretation of our findings is therefore preliminary. To date, very few neuroimaging studies of navigation have reported activity in the anterior part of the parahippocampal cortex (Parslow et al., 2005; Spiers and Maguire, 2006). Animal and human studies as well as theoretical models suggest that the parahippocampal cortex generates a representation of the environmental layout (Bird and Burgess, 2008; Moscovitch et al., 2005). Furthermore, spatial memory and associations and retrieval of indirect spatial relationships all engage the anterior parahippocampal cortex (Ekstrom and Bookheimer, 2007; Epstein, 2008; Preston et al., 2004). The increased activity in anterior parahippocampal cortex during the initial phase suggests that the anterior parahippocampal cortex provides a representation of the virtual environment at large. The posterior parahippocampus cortex was, however, active throughout navigation and in all conditions, underscoring the perceptual role of this region (Preston et al., 2004).

In summary, our results demonstrate that successful navigation requires dynamic recruitment of MTL subregions as navigation progresses from self-localization, target localization and navigational planning to execution of the navigational plan. Furthermore, the current findings support a functional segregation between anterior and posterior MTL. The anterior MTL, including the anterior hippocampus, anterior parahippocampal cortex and entorhinal cortex, was specifically engaged in the initial phase of navigation, irrespective of upcoming navigational demands. Activation in the posterior MTL, including the posterior hippocampus and posterior parahippocampal cortex, persisted throughout the entire navigational period. These results suggest that the anterior MTL engendered a mental representation of the environment as a whole, including a global sketch of current position, target position and the path between these two locations. The finding that the initial, transient anterior hippocampal activity correlated with navigational success 15–20 s later in the navigation block underscores the importance of this region in providing a map and a plan leading to the target. Regions in the posterior MTL were activated throughout the period of navigation and could be involved in keeping track of current location within the environment. The current results are consistent with the functional segregation suggested by electrophysiological recordings in the rat hippocampus and describe a similar segregation in the parahippocampal cortex. Finally, this study demonstrated a specific role for the entorhinal cortex in the initial phase of navigation. Although the spatial functions of this region have received much attention in animal studies, its role in human navigation remains to be explored further.

Acknowledgments

This study was funded by the Norwegian University of Science and Technology (NTNU) and the Center of competence for fMRI, St. Olav's hospital. We would like to thank Dr. Michael H. Chappell for proofreading the manuscript.

References

Adcock, R., Thangavel, A., Whitfield-Gabrieli, S., Knutson, B., Gabrieli, J., 2006. Reward-motivated learning: mesolimbic activation precedes memory formation. Neuron 50, 507–517.
Addis, D.R., Pan, L., Vu, M.-A., Laiser, N., Schacter, D.L., 2009. Constructive episodic simulation of the future and the past: distinct subsystems of a core brain network mediate imagining and remembering. Neuropsychologia 47, 2222–2238.
Anderson, M., Ochsner, K., Kuhl, B., Cooper, J., Robertson, E., Gabrieli, S., Glover, G., Gabrieli, J., 2004. Neural systems underlying the suppression of unwanted memories. Am. Assoc. Adv. Sci. 232–235.
Antonova, E., Parslow, D., Brammer, M., Dawson, G.R., Jackson, S.H.D., Morris, R.G., 2009. Age-related neural activity during allocentric spatial memory. Memory 17, 125–143.
Avila, C., Barros-Loscertales, A., Forn, C., Mallo, R., Parcet, M., Belloch, V., Campos, S., Feliu-Tatay, R., Gonzalez-Darder, J., 2006. Memory lateralization with 2 functional MR imaging tasks in patients with lesions in the temporal lobe. Am. Soc. Neuroradiol. 498–503.
Bast, T., Wilson, I.A., Witter, M.P., Morris, R.G.M., 2009. From rapid place learning to behavioral performance: a key role for the intermediate hippocampus. PLoS Biol. 7, e1000089.
Bird, C.M., Burgess, N., 2008. The hippocampus and memory: insights from spatial processing. Nat. Rev. Neurosci. 9, 182–194.
Buffalo, E.A., Bellgowan, P.S.F., Martin, A., 2006. Distinct roles for medial temporal lobe structures in memory for objects and their locations. Learn. Mem. 13, 638–643.
Burgess, N., Maguire, E.A., O'Keefe, J., 2002. The human hippocampus and spatial and episodic memory. Neuron 35, 625–641.
Chai, X.J., Ofen, N., Jacobs, L.F., Gabrieli, J.D.E., 2010. Scene complexity: influence on perception, memory, and development in the medial temporal lobe. Front. Hum. Neurosci. 4.
Chen, N., Dickey, C., Yoo, S., Guttmann, C., Panych, L., 2003. Selection of voxel size and slice orientation for fMRI in the presence of susceptibility field gradients: application to imaging of the amygdala. Neuroimage 19, 817–825.
Derdikman, D., Whitlock, J.R., Tsao, A., Fyhn, M., Hafting, T., Moser, M.-B., Moser, E.I., 2009. Fragmentation of grid cell maps in a multicompartment environment. Nat. Neurosci. 12, 1325–1332.
Doeller, C.F., King, J.A., Burgess, N., 2008. Parallel striatal and hippocampal systems for landmarks and boundaries in spatial memory. Proc. Natl. Acad. Sci. 105, 5915–5920.
Doeller, C.F., Barry, C., Burgess, N., 2010. Evidence for grid cells in a human memory network. Nature 463, 657–661.
Eichenbaum, H., Lipton, P.A., 2008. Towards a functional organization of the medial temporal lobe memory system: role of the parahippocampal and medial entorhinal cortical areas. Hippocampus 18, 1314–1324.
Ekstrom, A.D., Bookheimer, S.Y., 2007. Spatial and temporal episodic memory retrieval recruit dissociable functional networks in the human brain. Learn. Mem. 14, 645–654.
Epstein, R.A., 2008. Parahippocampal and retrosplenial contributions to human spatial navigation. Trends Cogn. Sci. 12, 388–396.
Flitney, D., Webster, M., Patenaude, B., Seidman, L., Goldstein, J., Tordesillas Gutierrez, D., Eickhoff, S., Amunts, K., Zilles, K., Lancaster, J., 2007. Anatomical brain atlases and their application in the FSLView visualisation tool.
Fyhn, M., Molden, S., Witter, M., Moser, E., Moser, M., 2004. Spatial representation in the entorhinal cortex. Science 305, 1258–1264.
Ghaem, O., Mellet, E., Crivello, F., Tzourio, N., Mazoyer, B., Berthoz, A., Denis, M., 1997. Mental navigation along memorized routes activates the hippocampus, precuneus, and insula. Neuroreport 8, 739–744.
Giovanello, K.S., Schnyer, D., Verfaellie, M., 2009. Distinct hippocampal regions make unique contributions to relational memory. Hippocampus 19, 111–117.
Grön, G., Wunderlich, A., Spitzer, M., Tomczak, R., Riepe, M., 2000. Brain activation during human navigation: gender-different neural networks as substrate of performance. Nat. Neurosci. 3, 404–408.
Hassabis, D., Chu, C., Rees, G., Weiskopf, N., Molyneux, P.D., Maguire, E.A., 2009. Decoding neuronal ensembles in the human hippocampus. Curr. Biol. 19, 546–554.
Hölscher, C., Meilinger, T., Vrachliotis, G., Brösamle, M., Knauff, M., 2006. Up the down staircase: wayfinding strategies in multi-level buildings. J. Environ. Psychol. 26, 284–299.
Hu, D., Amsel, A., 1995. A simple test of the vicarious trial-and-error hypothesis of hippocampal function. Proc. Natl. Acad. Sci. 92, 5506–5509.
Iaria, G., Chen, J.-K., Guariglia, C., Ptito, A., Petrides, M., 2007. Retrosplenial and hippocampal brain regions in human navigation: complementary functional contributions to the formation and use of cognitive maps. Eur. J. Neurosci. 25, 890–899.

Iaria, G., Fox, C.J., Chen, J.-K., Petrides, M., Barton, J.J.S., 2008. Detection of unexpected events during spatial navigation in humans: bottom-up attentional system and neural mechanisms. Eur. J. Neurosci. 27, 1017–1025.
Insausti, R., Juottonen, K., Soininen, H., Insausti, A., Partanen, K., Vainio, P., Laakso, M., Pitkanen, A., 1998. MR volumetric analysis of the human entorhinal, perirhinal, and temporopolar cortices. Am. J. Neuroradiol. 19, 659–671.
Janzen, G., Weststeijn, C., 2007. Neural representation of object location and route direction: an event-related fMRI study. Brain Res. 1165, 116–125.
Jeffery, K., 2007. Self-localization and the entorhinal–hippocampal system. Curr. Opin. Neurobiol. 17, 684–691.
Johnsrude, I., Owen, A., Crane, J., Milner, B., Evans, A., 1999. A cognitive activation study of memory for spatialrelationships. Neuropsychologia 37, 829–841.
Jordan, K., Schadow, J., Wuestenberg, T., Heinze, H.-J., Jäncke, L., 2004. Different cortical activations for subjects using allocentric or egocentric strategies in a virtual navigation task. Neuroreport 15, 135–140.
Jung, M., Wiener, S., McNaughton, B., 1994. Comparison of spatial firing characteristics of units in dorsal and ventral hippocampus of the rat. J. Neurosci. 14, 7347–7356.
Kirwan, C.B., Stark, C.E.L., 2004. Medial temporal lobe activation during encoding and retrieval of novel face-name pairs. Hippocampus 14, 919–930.
Kjelstrup, K.B., Solstad, T., Brun, V.H., Hafting, T., Leutgeb, S., Witter, M.P., Moser, E.I., Moser, M.-B., 2008. Finite scale of spatial representation in the hippocampus. Science 321, 140–143.
Kumaran, D., Maguire, E., 2005. The human hippocampus: cognitive maps or relational memory? J. Neurosci. 25, 7254–7259.
Lipton, P.A., White, J.A., Eichenbaum, H., 2007. Disambiguation of overlapping experiences by neurons in the medial entorhinal cortex. J. Neurosci. 27, 5787–5795.
Litman, L., Awipi, T., Davachi, L., 2009. Category-specificity in the human medial temporal lobe cortex. Hippocampus 19, 308–319.
Mellet, E., Bricogne, S., Tzourio-Mazoyer, N., Ghaem, O., Petit, L., Zago, L., Etard, O., Berthoz, A., Mazoyer, B., Denis, M., 2000. Neural correlates of topographic mental exploration: the impact of route versus survey perspective learning. Neuroimage 12, 588–600.
Miller, E., Cohen, J., 2003. An integrative theory of prefrontal cortex function.
Morris, R., 1984. Developments of a water-maze procedure for studying spatial learning in the rat. J. Neurosci. Methods 11, 47–60.
Moscovitch, M., Rosenbaum, R.S., Gilboa, A., Addis, D.R., Westmacott, R., Grady, C., McAndrews, M.P., Levine, B., Black, S., Winocur, G., Nadel, L., 2005. Functional neuroanatomy of remote episodic, semantic and spatial memory: a unified account based on multiple trace theory. J. Anat. 207, 35–66.
Moser, M.-B., Moser, E.I., 1998. Functional differentiation in the hippocampus. Hippocampus 8, 608–619.
Moser, E.I., Kropff, E., Moser, M.-B., 2008. Place cells, grid cells, and the brain's spatial representation system. Ann. Rev. Neurosci. 31, 69–89.
Mou, W., McNamara, T., Valiquette, C., Rump, B., 2004. Allocentric and egocentric updating of spatial memories. J. Exp. Psychol. Learn. Mem. Cogn. 30, 142–157.
Ohnishi, T., Matsuda, H., Hirakata, M., Ugawa, Y., 2006. Navigation ability dependent neural activation in the human brain: an fMRI study. Neurosci. Res. 55, 361–369.
Ojemann, J., Akbudak, E., Snyder, A., McKinstry, R., Raichle, M., Conturo, T., 1997. Anatomic localization and quantitative analysis of gradient refocused echo-planar fMRI susceptibility artifacts. Neuroimage 6, 156–167.
Owen, A.M., Milner, B., Petrides, M., Evans, A.C., 1996. A specific role for the right parahippocampal gyrus in the retrieval of object–location: a positron emission tomography study. J. Cogn. Neurosci. 8, 588–602.
Parslow, D., Morris, R., Fleminger, S., Rahman, Q., Abrahams, S., Recce, M., 2005. Allocentric spatial memory in humans with hippocampal lesions. Acta Psychol. 118, 123–147.
Peigneux, P., Laureys, S., Fuchs, S., Collette, F., Perrin, F., Reggers, J., Phillips, C., Degueldre, C., Del Fiore, G., Aerts, J., 2004. Are spatial memories strengthened in the human hippocampus during slow wave sleep? Neuron 44, 535–545.
Preston, A., Shrager, Y., Dudukovic, N., Gabrieli, J., 2004. Hippocampal contribution to the novel use of relational information in declarative memory. Hippocampus 14, 148–152.
Rauchs, G., Orban, P., Balteau, E., Schmidt, C., Degueldre, C., Luxen, A., Maquet, P., Peigneux, P., 2008. Partially segregated neural networks for spatial and contextual memory in virtual navigation. Hippocampus 18, 503–518.
Royer, S., Sirota, A., Patel, J., Buzsaki, G., 2010. Distinct representations and theta dynamics in dorsal and ventral hippocampus. J. Neurosci. 30, 1777–1787.
Schacter, D.L., Wagner, A.D., 1999. Medial temporal lobe activations in fMRI and PET studies of episodic encoding and retrieval. Hippocampus 9, 7–24.
Schmidt, D., Krause, B., Weiss, P., Fink, G., Shah, N., Amorim, M., Müller, H., Berthoz, A., 2007. Visuospatial working memory and changes of the point of view in 3D space. Neuroimage 36, 955–968.
Shipman, S., Astur, R., 2008. Factors affecting the hippocampal BOLD response during spatial memory. Behav. Brain Res. 187, 433–441.
Shrager, Y., Kirwan, C.B., Squire, L.R., 2008. Neural basis of the cognitive map: path integration does not require hippocampus or entorhinal cortex. Proc. Natl. Acad. Sci. 105, 12034–12038.
Slater, M., Usoh, M., Steed, A., 1995. Taking steps: the influence of a walking technique on presence in virtual reality. ACM Trans. Comput. Hum. Interact. (TOCHI) 2, 201–219.
Sommer, T., Rose, M., Weiller, C., Büchel, C., 2005. Contributions of occipital, parietal and parahippocampal cortex to encoding of object–location associations. Neuropsychologia 43, 732–743.
Spiers, H.J., Maguire, E.A., 2006. Thoughts, behaviour, and brain dynamics during navigation in the real world. Neuroimage 31, 1826–1840.
Spiers, H.J., Maguire, E.A., 2007a. A navigational guidance system in the human brain. Hippocampus 17, 618–626.
Spiers, H.J., Maguire, E.A., 2007b. The neuroscience of remote spatial memory: a tale of two cities. Neuroscience 149, 7–27.
Spiers, H., Maguire, E., 2008. The dynamic nature of cognition during wayfinding. J. Environ. Psychol. 28, 232–249.
Suzuki, W., Miller, E., Desimone, R., 1997. Object and place memory in the macaque entorhinal cortex. J. Neurophysiol. 78, 1062–1081.
Szpunar, K.K., Watson, J.M., McDermott, K.B., 2007. Neural substrates of envisioning the future. Proc. Natl. Acad. Sci. 104, 642–647.
Tyler, L., Stamatakis, E., Bright, P., Acres, K., Abdallah, S., Rodd, J., Moss, H., 2004. Processing objects at different levels of specificity. J. Cogn. Neurosci. 16, 351–362.
Wolbers, T., Wiener, J.M., Mallot, H.A., Buchel, C., 2007. Differential recruitment of the hippocampus, medial prefrontal cortex, and the human motion complex during path integration in humans. J. Neurosci. 27, 9408–9416.